



Thermally-Stable Passive Wireless Antenna Sensor for Strain Sensing

Dan Li¹, Yang Wang^{1,2,*}

¹ School of Civil and Environmental Engineering, Georgia Institute of Technology, Atlanta, GA 30332, USA

² School of Electrical and Computing Engineering, Georgia Institute of Technology, Atlanta, GA 30332, USA

*yang.wang@ce.gatech.edu

Abstract

Passive wireless antenna sensors have been studied in recent years as a novel approach for strain sensing. Electromagnetic resonance frequency of the antenna sensor, which is bonded on a base structural surface like a strain gage, depends on antenna dimension. When the dimension changes due to strain in the base structure, the wirelessly identified resonance frequency shift can be used to estimate the strain in the structure. Due to the multi-physics nature, both mechanical and dielectric properties of the antenna affect the resonance frequency. One drawback of previous antenna sensors is the relatively large resonance frequency fluctuation due to temperature change. This paper investigates a new patch antenna sensor that performs more stably under thermal influence. Thermal influence on the new patch antenna sensor is investigated through a day-long outdoor test. Multi-physics simulation is performed to verify that the antenna resonance frequency changes with strain. The strain sensing performance of the antenna sensor is finally validated through laboratory compression test.

1. Introduction

As core components in structural health monitoring (SHM), sensors provide important diagnostic data of structures. Among many new sensing technologies, passive wireless antenna sensors are known for their simplicity. Besides achieving wireless communication, researchers have harnessed patch antennas to measure structural strain through the antenna resonance frequency change. For example, Deshmukh and Huang (2010) investigated the potential of a rectangular patch antenna for strain measurement. Daliri *et al.* (2012) proposed a circular patch antenna sensor for measuring strain along different directions. Later, radio frequency identification (RFID) technology has been incorporated in the antenna sensor design to increase the interrogation distance and improve the measurement reliability (Yi *et al.*, 2011; Yi *et al.*, 2016).

Strain sensing performance of those antenna sensor have been investigated through both numerical simulation and laboratory experiments. However, besides structural strain, other environmental disturbances, such as temperature fluctuation, can also result in the resonance frequency change of the antenna. A large frequency change due to temperature fluctuation can be difficult to distinguish from strain effects. To reduce temperature effect on resonance frequency, this research investigates the performance of a thermally-stable passive wireless antenna sensor.

In this research, thermal influence on antenna sensors is investigated through a day-long outdoor test. The strain sensing performance of a thermally-stable passive wireless antenna sensor is studied through both multi-physics simulation and laboratory compression test. The paper is organized as follows. Section 2 introduces the strain sensing mechanism of an antenna sensor and two designs of the RFID-based passive antenna sensor. Section 3 discusses the thermal influences on both antenna sensors. Section 4 describes the multi-physics simulation on the strain sensing performance of the new design of antenna sensor. Section 5 presents the compression test on the antenna sensor. Finally, a summary and conclusion are provided.

2. Strain sensing mechanism

According to electromagnetic theory, the resonance frequency of an antenna at certain temperature T is given by:

$$f_{R0}(T) = \frac{c}{2L\sqrt{\beta_{r,eff}(T)}} \quad (1)$$

where c is the speed of light; L is the length of the electrical current path; $\beta_{r,eff}(T)$ is the effective dielectric constant of the substrate which depends on environmental temperature T .

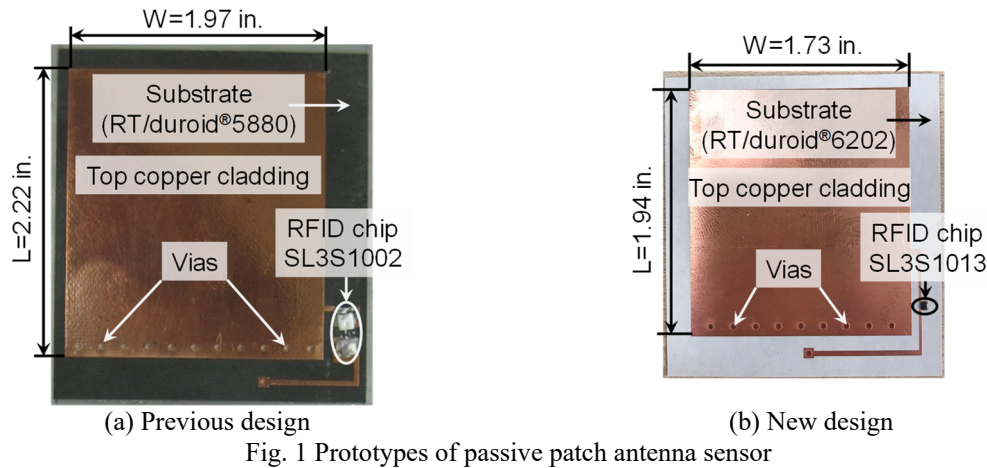
When longitudinal strain ϵ is applied on the antenna sensor, the length of the total current path changes from L to $L(1 + \epsilon)$. In civil structural applications, the dimensionless ϵ is usually on the order of 10^{-5} (10 micro-strain) to 10^{-3} (1,000 micro-strain). If the dielectric constant of the substrate $\beta_{r,eff}(T)$ remains as constant, the change of the resonance frequency $\Delta f(T)$ due to strain ϵ can be obtained as:

$$\Delta f(T) = f_{R\epsilon}(T) - f_{R0}(T) = \frac{f_{R0}(T)}{1 + \epsilon} - f_{R0}(T) \approx -f_{R0}(T)\epsilon = S(T)\epsilon \quad (2)$$

Here $S(T)$ is the theoretical strain sensitivity of the antenna sensor at temperature T . Thus, the antenna sensor can measure the strain by detecting the shift of its resonance frequency:

$$\epsilon = \frac{\Delta f(T)}{S(T)} \quad (3)$$

Different prototypes of passive patch antenna sensor have been proposed to measure strain wirelessly. Fig. 1 (a) and (b) show the designs of two passive patch antenna sensors. Both sensors have copper cladding and RFID chips mounted on the top side of the substrates. Vias connect the top copper cladding to the ground plane of each sensor. The main difference between these two sensors is the substrate material. Previous design (Fig. 1 (a)) of antenna sensor with Rogers RT/duroid[®] 5880 substrate is sensitive to temperature change. Laboratory experiments have shown that under temperature fluctuation, the previous design undergoes large resonance frequency change due to its large dielectric constant variation (Yi *et al.*, 2012). The large dielectric constant variation would result in difficulty for the sensor to estimate the structural strain from its resonance frequency change. To improve sensor reliability when temperature fluctuates, a thermally-stable substrate material RT/duroid[®] 6202 is chosen to upgrade the antenna sensor. In addition, a new

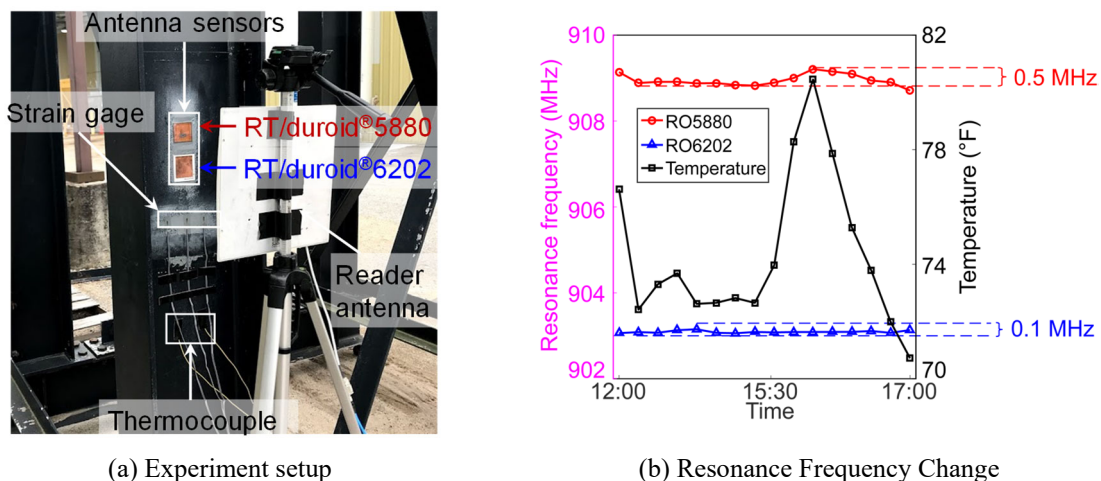


RFID chip with much smaller footprint is adopted. A new version of passive patch antenna sensor is designed according to the dielectric constant of the substrate and the impedance of the RFID chip (Fig. 1 (b)).

3. Outdoor temperature test

A day-long outdoor temperature test is conducted to study the influence of the temperature fluctuation on the resonance frequency of the antenna sensors. Fig. 2 (a) shows the outdoor experiment setup. Two antenna sensors, one with RT/duroid® 5880 substrate and the other with RT/duroid® 6202 substrate, are installed on the web surface of a steel I-section column. Metal foil strain gages are installed to measure the temperature induced strain on the steel column surface. To keep track of temperature fluctuations in the field, two thermocouples are installed near the sensors. An interrogation reader antenna is placed 12 in. away from the antenna sensor for wireless communication.

The outdoor test starts at noon with environmental temperature at around 76 °F. The temperature is measured every 20 minutes until 17:00. The temperature fluctuation is plotted in the Fig. 2 (b).



The highest temperature is around 80 °F and the lowest temperature is around 70 °F. At each time step, interrogation power threshold is measured for both patch antenna sensors. To reduce measurement noise, the reader antenna sweeps the target frequency span five times for each measurement. Resonance frequencies of both patch antenna sensors are extracted from the average interrogation power threshold curves and shown in Fig. 2 (b). A total of about 0.5 MHz resonance frequency change is observed on patch antenna sensor with RT/duroid® 5880 substrate during the test. Meanwhile, the patch antenna sensor with RT/duroid® 6202 substrate shows a total about 0.1 MHz resonance frequency change, which is much less than that of the previous design with RT/duroid® 5880 substrate.

4. Multi-physics simulation

To accurately describe both mechanical and electromagnetic behaviors of the patch antenna sensor, a multi-physics coupled simulation approach is adopted. The patch antenna sensor is modeled using ANSYS software package. Fig. 3 (a) shows the finite element model. The antenna sensor is attached at the center of a tapered aluminum plate. Above the antenna sensor, an air layer is built to consider the fringing effect. Shell elements are utilized to model the copper cladding on both top and bottom sides of the antenna sensor. Solid elements are utilized to model the substrate layer, the air layer, and the aluminum specimen. For simplicity, the bonding effect between the antenna sensor and the aluminum plate is considered ideal in the simulation, i.e. the bottom copper cladding shares the same finite element nodes with the corresponding area of the top surface of the aluminum plate.

To generate three-point bending in the mechanical simulation, the bottom nodes of the aluminum specimen fix the translational DOFs along x , y , and z . Two corners in the middle part of the aluminum specimen are fixed along z -direction and free to move in x and y . Forces along z -direction are applied on the top nodes of the aluminum specimen to generate compression strain

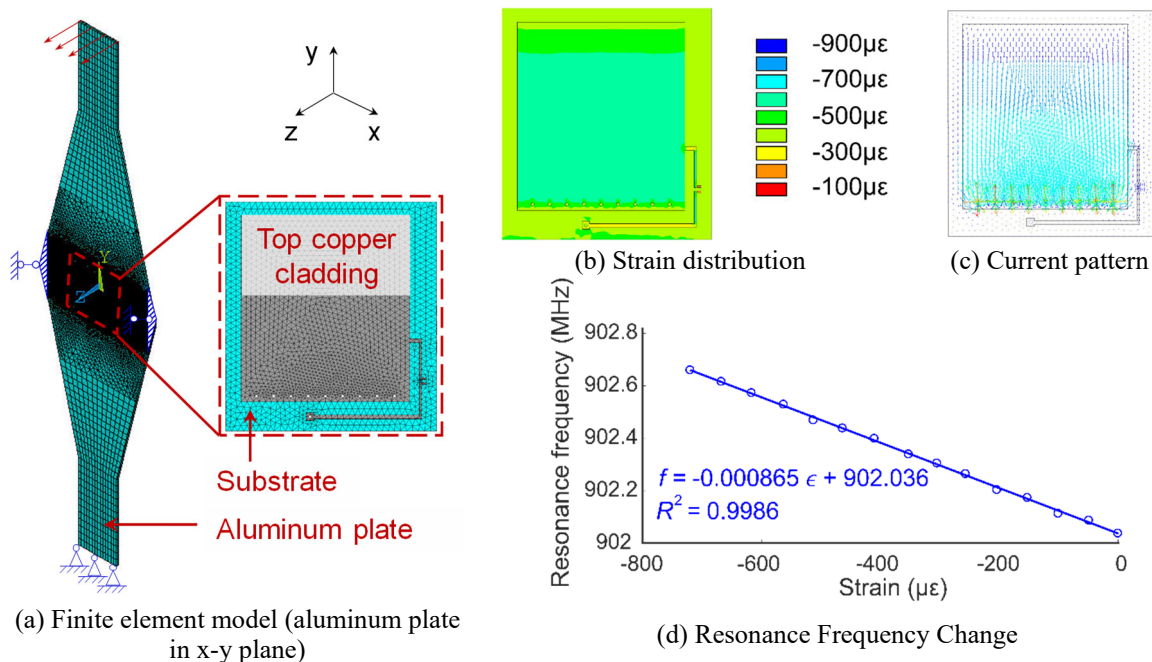


Fig. 3 Multi-physics simulation on patch antenna sensor

the in the sensor area. From 0 to 700 $\mu\epsilon$ with 50 $\mu\epsilon$ increment, 15 strain levels in total are simulated. Fig. 3 (b) shows the strain distribution along y -direction on the antenna sensor at strain level of 700 $\mu\epsilon$. Approximately uniform strain distribution is achieved on the antenna sensor. After the mechanical simulation at each strain level, the deformed finite element model is used for electromagnetic simulation to calculate the resonance frequency of the antenna sensor. Fig. 3 (c) illustrates the current pattern on the antenna sensor at its resonant mode. Using this multi-physics simulation approach, the resonance frequency of deformed antenna sensor at each strain level can be accurately calculated. Fig. 3 (d) plots the resonance frequency change along with the compression strain. Linear regression is applied on these data points, and the strain sensitivity is calculated as $-865 \text{ Hz}/\mu\epsilon$.

5. Compression test

Laboratory compression test is conducted to investigate the strain sensing performance of the patch antenna sensor. Fig. 4 (a) shows the setup of the compression test. A three-point bending device is designed and utilized to apply compression strain on the patch antenna sensor. The patch antenna sensor and reference metal foil strain gages are installed in the middle of tapered aluminum specimen. The interrogation distance between the patch antenna sensor and the reader antenna is set as 18 in. From 0 to 700 $\mu\epsilon$, the load is adjusted so that approximately a 50 $\mu\epsilon$ increment is obtained at each loading step. The interrogation power threshold of the patch antenna sensor is measured at each loading step. To reduce measurement noise, five frequency sweeps are conducted for each measurement. The average interrogation power threshold are plotted in Fig. 4 (b). For clarity, only four representative strain levels are shown. Resonance frequency of the patch antenna sensor at each strain level is then determined by peak picking of each average interrogation power

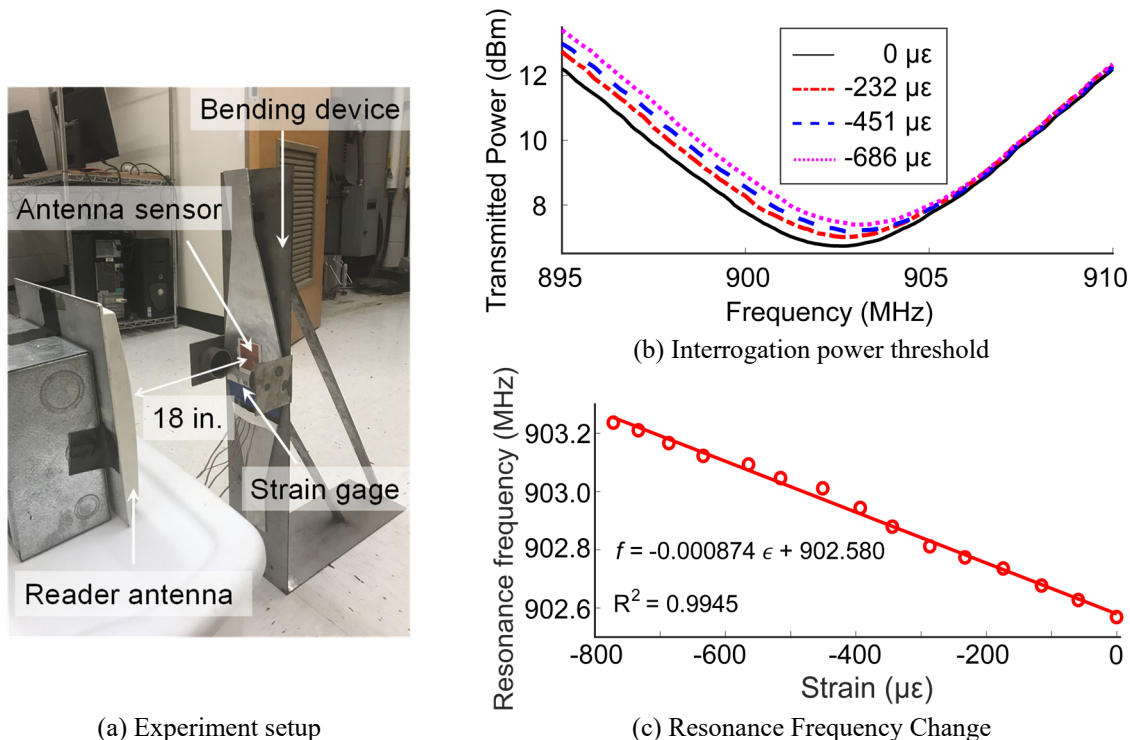


Fig. 4 Compression test

threshold curve. As expected, the resonance frequency increases as the compression strain increases. Fig. 4 (c) plots the resonance frequency change with the strain. Linear regression is applied on these data points, and the strain sensitivity is calculated as $-874 \text{ Hz}/\mu\epsilon$, which is close to the simulated result $-865 \text{ Hz}/\mu\epsilon$ as shown in Section 4. In addition, The coefficient of determination is 0.9945, confirming the approximately linear relationship between frequency change and strain.

6. Conclusion

This research presents the strain sensing performance of a thermally-stable passive patch antenna sensor. Extensive numerical simulation and laboratory tests have been conducted to characterize the performance of the passive wireless antenna sensor with RT/duroid[®] 6202 substrate. The patch antenna sensor with RT/duroid[®] 6202 substrate is shown to be more stable under outdoor environment disturbance compared with previous sensor with substrate material RT/duroid[®] 5880. Multi-physics simulation can accurately capture mechanical and electromagnetic behaviors of the patch antenna sensor. Compression test is conducted using a three-point bending setup to verify the strain sensing performance of the patch antenna sensor. Both numerical simulation and laboratory test show that the patch antenna sensor is capable of estimating small strain changes on the base structure.

Acknowledgement

This material is based upon work sponsored by the INSPIRE University Transportation Center through USDOT/OST-R grant #69A3551747126. Any opinions, findings, and conclusions or recommendations expressed in this publication are those of the authors and do not necessarily reflect the view of the sponsors.

References

- Daliri, A., Galehdar, A., John, S., Wang, C. H., Towe, W. S. T., and Ghorbani, K. (2012). "Wireless strain measurement using circular microstrip patch antennas." *Sensors and Actuators A*, 184, 86-92.
- Deshmukh, S., and Huang, H. (2010). "Wireless interrogation of passive antenna sensors." *Meas. Sci. Technol.*, 21(3), 035201.
- Yi, X., Wu, T., Wang, Y., Leon, R. T., Tentzeris, M. M., and Lantz, G. (2011). "Passive wireless smart-skin sensor using RFID-based folded patch antennas." *Int. J. Smart Nano Mater*, 2(1), 22-38.
- Yi, X., Vyas, R., Cho, C., Fang, C.-H., Cooper, J., Wang, Y., Leon, R. T., and Tentzeris, M. M. (2012). "Thermal effects on a passive wireless antenna sensor for strain and crack sensing." *Proceedings of SPIE, Sensors and Smart Structures Technologies for Civil, Mechanical and Aerospace Systems*, San Diego, CA, USA, pp. 83450F
- Yi, X., Cho, C., Wang, Y., and Tentzeris, M. M. (2016). "Battery-free slotted patch antenna sensor for wireless strain and crack monitoring." *Smart Struct. Syst.*, 18(6), 1217-1231.



Assessing moisture content on the surface of mortar samples from hyperspectral imaging

Liang Fan, Abdullah Alhaj, Hongyan Ma, Genda Chen

¹*Department of Civil, Architectural and Environmental Engineering,
Missouri University of Science and Technology (S&T)
Rolla, MO, USA, Email: lf7h2@mst.edu*

Abstract

Hyperspectral imaging represents an electromagnetic spectrum for each pixel in the image of a structural surface. The characteristic wavelength of the spectrum at reflectance valleys or absorption peaks can be used as a spectral feature for certain chemical detection. In this study, spectral reflectance characteristics of mortar samples are extracted to assess the reduction of moisture on the surface of mortar samples during the cement hydration process. The test results indicate that the reflectance increases and the absorbance decreases because water is reacted and less light will be absorbed during the hydration process. The average absorbance between 1923 nm and 1983 nm in wavelength gradually decreases with the mortar curing time. This feature parameter can be used to evaluate the mortar hydration process.

1. Introduction

Concrete is the most widely used material in buildings, bridges, dams, tunnels, pavements, runways and roads due to its high durability and resistance to weathering and natural disasters. When concrete structures like pavements are built on site, usually a minimum curing period is required to ensure that the concrete can attain the specified compressive strength before the road is open to the traffic (ACI Committee 301, 1972). It is necessary to understand the minimum curing period of the concrete to reduce the economy cost caused by the shut-down of traffic. The pull off test and the maturity method are used to determine the strength of concrete in situ but both methods need to establish the reference curves. The concrete curing process occurs immediately after finishing. The cement hydration consumes free water in the pore solution and generates hydration products like C-S-H gel and calcium hydroxide (Liu et al., 2017). Therefore, the reduced moisture content can be used as a sign to predict the increase in the strength of concrete. Backscattered electron imaging has been used to study the free-water content in concrete through measuring the concrete porosity (Sahu et al., 2004; Wong et al., 2019). As this method can only be implemented in laboratory, other techniques are needed to determine the water content of concrete on site without destroying it.

Hyperspectral imaging has been utilized in mineral identification, vegetation classification, and natural resource exploration (Zaini et al., 2016; DeTar et al., 2008; Tian et al., 2012). These